Received: Added at production | Revised: Added at production | Accepted: Added at production

DOI: xxx/xxxx

ARTICLE TYPE

Inverse Gaussian Process Model with Frailty Term in Reliability Analysis

Lia H. M. Morita*[1] | Vera L. Tomazella[2] | Narayanaswamy Balakrishnan[3] | Pedro L. Ramos[4] | Paulo H. Ferreira[4] | Francisco Louzada[4]

[1]Department of Statistics, Federal University of Mato Grosso, Cuiabá, Mato Grosso, Brazil

[2]Department of Statistics, Federal University of São Carlos, São Carlos, São Paulo, Brazil

[3]Department of Mathematics and Statistics, McMaster University, Hamilton, Ontario, Canada

[4]Institute of Mathematical and Computer Sciences, University of São Paulo, São Carlos, São Paulo, Brazil

Correspondence

*Corresponding author name: Lia H. M. Morita. Email: liamorita@ufmt.br

Summary

Traditional reliability analysis techniques focus on the occurrence of failures over time. Nevertheless, in certain cases where the occurrence of failures is tiny or almost null, the estimation of the quantities that describe the failure process is compromised. In this context, we introduce a reliability model for systems adopting the degradation process using frailty. The evolved degradation model has as experimental data, not the failure, but a quality feature attached to it. Degradation analysis can provide information about the lifetime distribution components without actually observing failures. In this paper, we propose an inverse Gaussian process model with frailty as a possible tool to investigate the effect of unobserved covariates. Moreover, a comparative study with the classical inverse Gaussian process based on simulated data was performed, revealing that the asymptotic properties of the maximum likelihood estimators are compromised when the presence of frailty is ignored. The application was based on two real datasets in the literature, showing that the inverse Gaussian process frailty models are propitious to use, however gamma and inverse Gaussian distributions for frailty present similar results.

KEYWORDS:

Degradation analysis, inverse Gaussian process, frailty, LASER data, crack size data.

1 | INTRODUCTION

Highly reliable products show a few or no failures, therefore it is difficult or impossible to assess reliability using traditional life tests that register only time-to-failure. Nevertheless, when failure can be related directly to a quality feature over time, we then have the possibility of measuring degradation and use it to evaluate the product's reliability. The latent failure process' features can be accessed and inferences can be made about the implied lifetime distribution.

In reliability engineering, there are two main classes of models, namely, the threshold models and the shock models; the main difference between them is the way the failure is featured. In the threshold models, a component shows performance loss when its degradation level first reaches a certain threshold; such phenomenon is referred to as a soft failure, and the unit is generally switched off. In the shock models, a component is exposed to external shocks, and is able to survive or fail; the eventual failures are referred to as hard or traumatic failures, and the shocks generally occur according to a Poisson process whose intensity depends on degradation and environmental factors[1]. Within the class of threshold models, we can mention the general path models and the stochastic process models.

The degradation models based on stochastic processes are very intuitive once degradation is a continuous process of wear over time. Based on the assumption of additive accumulation of degradation, two classes of degradation models have been investigated in depth, namely, the Wiener and gamma processes. Various papers in the literature assume the degradation paths to follow the Wiener process, e.g., Doksum[2] used a Wiener process with accelerating factors to analyze degradation data, and Wang[3] presented a Wiener process with random effects for degradation data. In the Wiener process, the sample paths are not necessarily monotone, which might not be meaningful in many applications.

As an alternative, the gamma process is frequently assumed when monotonicity is needed. The gamma process is the limit of a compound Poisson process and the jump size complies with a specific distribution[4]. This interpretation underpins the gamma process as a suitable degradation model because many reliability engineers believe that degradation is often provoked by a series of external shocks, each with random and minor damage[5].

Another degradation model with monotone paths is the inverse Gaussian process (IGP) introduced by Wasan[6]. Some examples in the literature are: Wang and Xu[7], who proposed an IGP with random effects and covariates to account for heterogeneity. In their work, the authors incorporated the random effect into the model to represent the variability from unit to unit, that is, an IGP $\{Y(t);\ t \geq 0\}$ with mean function $\Delta(t)$ and scale parameter η, where η is considered unobserved random effect and belongs to gamma distribution. Ye and Chen[8] regarded the IGP as the limit of a compound Poisson process whose arrival rate goes to infinity while the jump size goes to zero in a certain way; they included a random drift in the mean function of the IGP, leading to individual degradation paths with different slopes. Peng[9] introduced a degradation model based on an inverse normal-gamma mixture of an IGP. Qin *et al.*[10] proposed an IGP-based model with a Bayesian approach to characterize the growth of metal loss corrosion defects on energy pipelines, whereby the measurement errors in the paths are considered. Liu *et al.*[11] developed a reliability model for systems with s-dependent degradation processes using copulas, whereby the degradation processes are s-dependent among each other and the marginal degradation process is modeled by an IGP with time-scale transformation and random drift to account for possible heterogeneity.

Reliability data analysis often leads to an apparent decreasing failure rate, which could be counterintuitive because of wear and aging effects. Proschan[12] pointed out that such observed decreasing rates could be caused by unobserved heterogeneity. In engineering approaches, there is heterogeneity, including the unit-to-unit variability, the variability in time-varying operating conditions, and the diversity of tasks and workloads of a system during its lifetime. The usual methods of analyzing this kind of data show some limits in cases with heterogeneity from the inner states or the external operating conditions of systems. For example, the performance degradation of a system is a result of interactions of both the inner deterioration and the working environment of this system, indicating a need for incorporating heterogeneity into degradation modeling to achieve a more accurate reliability estimation[13]. The concept of frailty provides a way to introduce random effects in the model to account for the association and unobserved heterogeneity. In its simplest form, a frailty is an unobserved random factor that modifies multiplicatively the hazard function or underlying intensity $h_0(t)$ of an individual or a group or cluster of individuals, in which the individual i is supposed to have death intensity $z_i h_0(t)$ at age t, where the random variable z_i (the "frailty") is assumed to follow some known distribution, e.g., gamma distribution[14]. The idea is that systems with high frailty values will have larger failure proneness than systems with low frailty values. It is assumed that the systems are independent and lifetimes from the same system are independent of each other. Intuitively, the variation between systems implies that the variation in the observed number of failures among the systems is larger than would be expected if the failure processes were identically distributed[15].

The frailty models are likely to be notably useful for modeling multivariate survival times, whether "serial" or "parallel"[16]. Hougaard[17] noticed the double role of the frailty distribution with finite mean in describing both non-proportionality and inter-class correlation. Unkel and Farrington[18] provided a worthwhile representation of bivariate current status data to make the selection easier of a frailty model. In the context of degradation analysis, we can mention interesting papers, e.g., Lin *et al.*[19] reported an accelerated failure time model with frailty for the analysis of locomotive wheel degradation under piecewise constant hazard rate and gamma frailty; and Lin and Asplund[20] presented a similar approach under Weibull baseline hazard rates. In these papers, the lifetime information was based on the pseudo lifetimes, which are obtained when we assume some standard form for the degradation rate, e.g. linear, exponential or power law.

Although the IGP is widely used in the literature, it is not common to find works that use this model in the context of frailty models. This motivated us to turn our attention to it. Differently from the approach proposed by Wang and Xu[7], the frailty model is a random-effects model for time-to-event data, where the random effect (the frailty) acts as a multiplicative effect on the baseline hazard function. In this context, we aim to propose a class of models based on IGP with frailty (IGP frailty models), where the frailty term expresses the variability between the components and the variability in the measurements of the same components. Besides, it can take into account important variables that cannot be observed or measured. There are advantages in

separating these sources of variability: heterogeneity can explain some unexpected results or give an alternative interpretation, for example, crossing-over or leveling-of effects of hazard functions.

In this work, we considered gamma and inverse Gaussian (IG) distributions for frailty. In the application with real datasets, the IGP-gamma and IGP-IG frailty models showed similar results, and we estimated the individual frailties, as well as the components' lifetime distribution via the proposed methodology.

The paper is organized as follows. Section 2 describes the IGP model. In Section 3, we introduce the IGP with frailty term, referred to as the IGP frailty model, in order to capture the variability among different units and within the same unit. In Section 4, we present a simulation study and in Section 5 we provide the application with two real datasets in the literature. Finally, in Section 6 we draw some conclusions followed by bibliographic references.

2 | INVERSE GAUSSIAN PROCESS MODEL

Let $\{D(t);\, t \geq 0\}$ denote an increasing continuous-time stochastic process. When a unit is subject to a degradation phenomenon and the probability distribution of the degradation increment $\Delta D(t) = D(t+\Delta t) - D(t)$ over a future time interval $\Delta(t) = (t, t+\Delta t)$ is assumed to depend only on the present and not on the past history, then the process is said to be Markovian. In other words, a Markov (or Markovian) process is a stochastic process whose future state is independent of its past given its present state (for further details on Markovian processes, see, e.g., Ibe[21,22]). Markovian processes include Brownian motion, Wiener, gamma and IG processes, among others.

The IGP is a continuous-time stochastic process $\{D(t);\, t \geq 0\}$ with mean function $g_\theta(t)$ and scale parameter η given by

$$D(t) \sim \text{IG}\left(g_\theta(t),\, \eta g_\theta^2(t)\right), \tag{1}$$

where $g_\theta(\cdot)$ is a monotone increasing function of time t indexed by the parameter vector $\boldsymbol{\theta}$, with $g_\theta(0) = 0$ and $\eta > 0$.

It has the following properties:

- $D(0) = 0$;
- The distribution of each increment $Y = \Delta D(t)$ in the time interval Δt is given by

$$Y \sim \text{IG}\left(\Delta g_\theta(t),\, \eta(\Delta g_\theta(t))^2\right), \quad \forall \Delta t \geq 0,$$

  where $\Delta g_\theta(t)$ is the increment of $g_\theta(t)$ in the time interval Δt;
- The increments are independent.

The function $g_\theta(t)$ has a meaningful interpretation - it is the mean function of IGP - and η is inversely proportional to the variance of IGP:

$$E[D(t)] = g_\theta(t) \quad \text{and} \quad Var[D(t)] = \frac{g_\theta(t)}{\eta}.$$

The cumulative distribution function (CDF) of the degradation increment Y in the time interval Δt is the probability of Y being lower than some $y > 0$, and comes directly from the CDF of the IG distribution:

$$\begin{aligned} F_{\text{IGP}}(y|\Delta g_\theta(t), \eta) &= F_{\text{IG}}(y|\mu = \Delta g_\theta(t), \lambda = \eta(\Delta g_\theta(t))^2) \\ &= \exp\left\{2\eta \Delta g_\theta(t)\right\} \Phi\left(-\sqrt{\frac{\eta}{y}}(y + \Delta g_\theta(t))\right) + \Phi\left(\sqrt{\frac{\eta}{y}}(y - \Delta g_\theta(t))\right), \end{aligned} \tag{2}$$

where $F_{\text{IG}}(\cdot)$ is the CDF of IG distribution:

$$F_{\text{IG}}(y|\mu, \lambda) = \exp\left\{\frac{2\lambda}{\mu}\right\} \Phi\left(-\sqrt{\frac{\lambda}{y}}\left(\frac{y}{\mu} + 1\right)\right) + \Phi\left(\sqrt{\frac{\lambda}{y}}\left(\frac{y}{\mu} - 1\right)\right),$$

with $\mu > 0$, $\lambda > 0$ and $\Phi(\cdot)$ is the standard normal CDF.

Thus, the reliability function of the degradation increment Y is interpreted as the probability of Y being higher than y and given by

$$R_{\text{IGP}}(y|\Delta g_\theta(t), \eta) = 1 - F_{\text{IGP}}(y|\Delta g_\theta(t), \eta). \tag{3}$$

The function (3) has an inverse relationship with the component reliability because the components with high degradation increments are likely to be less reliable and show early failures.

The probability density function (PDF) is given by

$$\begin{aligned} f_{\text{IGP}}(y|\Delta g_\theta(t),\eta) &= f_{\text{IG}}(y|\mu=\Delta g_\theta(t),\lambda=\eta(\Delta g_\theta(t))^2) \\ &= \sqrt{\frac{\eta}{2\pi y^3}}\Delta g_\theta(t)\exp\left\{-\frac{\eta(y-\Delta g_\theta(t))^2}{2y}\right\}, \end{aligned}$$

where $f_{\text{IG}}(y|\mu,\lambda)=\sqrt{\frac{\lambda}{2\pi y^3}}\exp\left\{-\frac{\lambda(y-\mu)^2}{2\mu^2 y}\right\}$ is the PDF of IG distribution.

Finally, the intensity function and the cumulative intensity function are given, respectively, by

$$h_{\text{IGP}}(y|\Delta g_\theta(t),\eta)=\frac{f_{\text{IGP}}(y|\Delta g_\theta(t),\eta)}{R_{\text{IGP}}(y|\Delta g_\theta(t),\eta)} \tag{4}$$

and

$$H_{\text{IGP}}(y|\Delta g_\theta(t),\eta)=\int_0^y h_{\text{IGP}}(u|\Delta g_\theta(t),\eta)du=-\log\left(R_{\text{IGP}}(y|\Delta g_\theta(t),\eta)\right). \tag{5}$$

2.1 | Lifetime distribution

In many engineering applications, the failure time T for an item is defined as the time upon which the degradation path $D(t)$ first reaches a pre-determined threshold ρ, which must be fixed in general:

$$T=\inf\{t\geq 0 \mid D(t)\geq\rho\}. \tag{6}$$

Considering (6), the lifetime CDF is obtained directly from using the fact that the cumulative degradation $D(t)$ is the degradation increment in the time interval $[0,t]$ and $g_\theta(t)$ is the increment of the mean function of IGP in this time interval:

$$\begin{aligned} F_{T_{\text{IGP}}}(t) &= 1-F_{\text{IGP}}(y=\rho|g_\theta(t),\eta) \\ &= \Phi\left(-\sqrt{\frac{\eta}{\rho}}(\rho-g_\theta(t))\right)-\exp\left\{2\eta g_\theta(t)\right\}\Phi\left(-\sqrt{\frac{\eta}{\rho}}(\rho+g_\theta(t))\right), \end{aligned}$$

where $F_{\text{IGP}}(\cdot)$ is as given in (2).

Therefore, the lifetime PDF is given by

$$\begin{aligned} f_{T_{\text{IGP}}}(t) &= \frac{\partial F_{T_{\text{IGP}}}(t)}{\partial t} \\ &= \phi\left(-\sqrt{\frac{\eta}{\rho}}(\rho-g_\theta(t))\right)\frac{\partial g_\theta(t)}{\partial t}\sqrt{\frac{\eta}{\rho}}-\exp\left\{2\eta g_\theta(t)\right\}\Phi\left(-\sqrt{\frac{\eta}{\rho}}(\rho+g_\theta(t))\right)\frac{2\eta\partial g_\theta(t)}{\partial t} \\ &\quad+\exp\left\{2\eta g_\theta(t)\right\}\phi\left(-\sqrt{\frac{\eta}{\rho}}(\rho+g_\theta(t))\right)\frac{\partial g_\theta(t)}{\partial t}\sqrt{\frac{\eta}{\rho}}, \end{aligned} \tag{7}$$

where $\phi(\cdot)$ is the standard normal PDF.

The distribution of the first passage time T plays an important role in predicting remaining useful life as well as in determining optimal maintenance strategies[23].

3 | INVERSE GAUSSIAN PROCESS MODEL WITH FRAILTY TERM

In reliability analysis, incorporating the unobserved heterogeneity among experimental units is called frailty. In this work, the frailty term will act in the reliability of the equipment as an unobserved covariate, thus helping to assess the population reliability function.

Clayton[24] introduced a frailty term in the Cox model[25] in a multiplicative way, i.e., the random variable representing the frailty, z, acts multiplicatively in the baseline hazard function $h_0(t)$, then

$$h(t|z)=zh_0(t), \tag{8}$$

where z is a positive unobservable random variable (called frailty) that increases the individual hazard if $z>1$ or decreases it if $z<1$. Intuitively, the greater the individual frailty, the greater the probability of failure[14].

The individual hazard function $h(t|z)$ is interpreted as the conditional hazard function given z. Hence, the reliability function conditional to z is given by

$$R(t|z) = \exp\left\{-\int_0^t h(s|z)ds\right\} = \exp\left\{-z\int_0^t h_0(s)ds\right\} = \exp\left\{-zH_0(t)\right\}, \tag{9}$$

where $H_0(t)$ is the cumulative baseline hazard function at time t.

The unconditional reliability function $R(t)$ is obtained by integrating (9) out the frailty component by means of the frailty PDF $f_{\boldsymbol{\alpha}}(z)$, indexed by the parameter vector $\boldsymbol{\alpha}$:

$$R(t) = \int_0^\infty R(t|z)f_{\boldsymbol{\alpha}}(z)dz = \int_0^\infty \exp\left\{-zH_0(t)\right\} f_{\boldsymbol{\alpha}}(z)dz, \tag{10}$$

which can be obtained by the Laplace transform[26].

In this study, we consider an alternative to the IGP model with random effects, in which the random effect, called frailty, is incorporated in the intensity function of the IGP model.

The building of a frailty IGP grounded on the multiplicative frailty model (8) may have some peculiarities. First, the intensity function describes the intensity over the degradation increments, which is different from the hazard rate in lifetime analysis. Second, the frailty must possess an inversely proportional relationship with intensity, i.e., the higher the frailty value, the greater the probability of large degradation increments related to failure. Thus, for each unit i, the degradation increment Y in the time interval Δt has its intensity function defined as

$$h_i(y|\Delta g_{\boldsymbol{\theta}}(t), \eta, z_i) = \frac{1}{z_i} \times h_{\text{IGP}}(y|\Delta g_{\boldsymbol{\theta}}(t), \eta), \tag{11}$$

where $h_{\text{IGP}}(y|\Delta g_{\boldsymbol{\theta}}(t), \eta)$ is referred to as the baseline intensity function with the expression as given in (4), and $\Delta g_{\boldsymbol{\theta}}(t)$ and η are as given in Section 2.

Equation (11) can be easily understood as follows:

- The lower the z_i, the greater the term $1/z_i$, then the frailty term acts increasing the conditional hazard function for each individual. This means that the resulting function assumes high values at the beginning of the curve, hindering the occurrence of high values (y) at the end of the curve. As a result, the less fragile components will probably take a long time to reach the threshold related to failure.

- Inversely, the higher the z_i, the lower the term $1/z_i$, which means that the frailty term acts decreasing the conditional hazard function for each individual. Therefore, the resulting function assumes low values at the beginning of the curve, facilitating the appearance of high degradation values to the right of the curve. Accordingly, the most fragile components are prone to attain the threshold early.

The conditional reliability function for the IGP frailty model (11) is given by

$$R_i(y|\Delta g_{\boldsymbol{\theta}}(t), \eta, z_i) = \left[R_{\text{IGP}}(y|\Delta g_{\boldsymbol{\theta}}(t), \eta)\right]^{\frac{1}{z_i}},$$

where $R_{\text{IGP}}(y|\Delta g_{\boldsymbol{\theta}}(t), \eta)$ is as given in (3).

Figure 1 exhibits three degradation paths for three different z_i values. The plot consists of 3 units which are evaluated from 0 up to 4 time units with 10 equidistant intervals. The mean function for IGP was set as $g_{\boldsymbol{\theta}}(t) = \theta t$, $\theta > 0$, and the parameter values are shown in the plot. For the sake of analysis, the z_i values are fixed instead of random, and we see that large degradation values are related to high frailty values.

3.1 | Unconditional reliability function, CDF and PDF of the degradation increments

The unconditional reliability function for increment Y in the time interval Δt is similar to (10) with some modification, i.e., the lifetime values are replaced by the degradation increments and the contribution of the frailty term in the exponent is $\frac{1}{z_i}$ rather

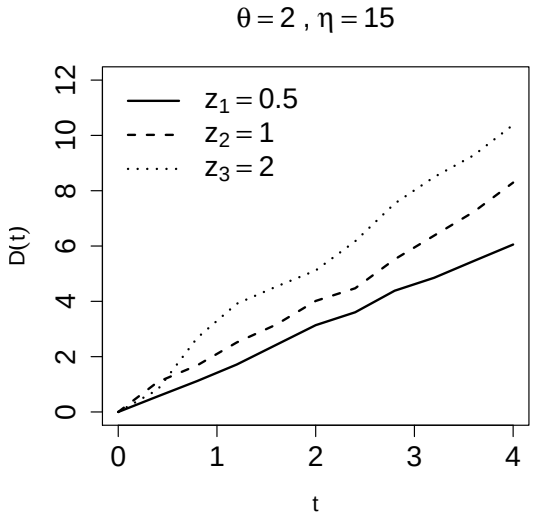

FIGURE 1 The degradation paths for three different z_i values, which consist of 3 units evaluated from 0 up to 4 time units with 10 equidistant intervals.

than z_i:

$$\begin{aligned} R(y|\Delta g_{\boldsymbol{\theta}}(t),\eta,\boldsymbol{\alpha}) &= \int_0^\infty R_i(y|\Delta g_{\boldsymbol{\theta}}(t),\eta,z_i) f_{\boldsymbol{\alpha}}(z_i) dz_i \\ &= \int_0^\infty \exp\left\{-\frac{1}{z_i} H_{\text{IGP}}(y|\Delta g_{\boldsymbol{\theta}}(t),\eta)\right\} f_{\boldsymbol{\alpha}}(z_i) dz_i. \end{aligned} \tag{12}$$

Notice that (12) depends on $\boldsymbol{\alpha}$, which means that marginalization incorporates the frailty information in the reliability function via the parameter vector $\boldsymbol{\alpha}$. From (12) and relation (5), we can observe the next cases:

- **Case 1:** For too large y values, $R_{\text{IGP}}(y|\Delta g_{\boldsymbol{\theta}}(t),\eta) \approx 0$. Hence, $H_{\text{IGP}}(y|\Delta g_{\boldsymbol{\theta}}(t),\eta) \approx \infty$.

- **Case 2:** For too small y values, $R_{\text{IGP}}(y|\Delta g_{\boldsymbol{\theta}}(t),\eta) \approx 1$. Thus, $H_{\text{IGP}}(y|\Delta g_{\boldsymbol{\theta}}(t),\eta) \approx 0$.

Based on these situations, we rewrite (12) as

$$R(y|\Delta g_{\boldsymbol{\theta}}(t),\eta,\boldsymbol{\alpha}) = \begin{cases} 0, \text{ if } R_{\text{IGP}}(y|\Delta g_{\boldsymbol{\theta}}(t),\eta) = 0, \\ \int_0^\infty \exp\left\{-\frac{1}{z_i} H_{\text{IGP}}(y|\Delta g_{\boldsymbol{\theta}}(t),\eta)\right\} f_{\boldsymbol{\alpha}}(z) dz, \text{ if } 0 < R_{\text{IGP}}(y|\Delta g_{\boldsymbol{\theta}}(t),\eta) < 1, \\ 1, \text{ if } R_{\text{IGP}}(y|\Delta g_{\boldsymbol{\theta}}(t),\eta) = 1. \end{cases} \tag{13}$$

The formula (13) based on different scenarios intends to avoid indeterminate values occurring in simulated studies. Besides, the integral in (13) can be solved analytically or numerically, depending on frailty distribution.

Thus, the unconditional CDF is given by

$$F(y|\Delta g_{\boldsymbol{\theta}}(t),\eta,\boldsymbol{\alpha}) = 1 - R(y|\Delta g_{\boldsymbol{\theta}}(t),\eta,\boldsymbol{\alpha}). \tag{14}$$

From (14), we conclude that IGP frailty model also has monotone behavior, since $F_{\text{IGP}}(y|\Delta g_{\boldsymbol{\theta}}(t),\eta)$ is positive only for positive y values, otherwise it is null.

Finally, the unconditional PDF is the derivative of (14) with respect to y:

$$f(y|\Delta g_{\boldsymbol{\theta}}(t),\eta,\boldsymbol{\alpha}) = \begin{cases} 0, \text{ if } f_{\text{IGP}}(y|\Delta g_{\boldsymbol{\theta}}(t),\eta) = 0, \\ \dfrac{\partial F(y|\Delta g_{\boldsymbol{\theta}}(t),\eta,\boldsymbol{\alpha})}{\partial y}, \text{ otherwise.} \end{cases}$$

Considering (6), the lifetime CDF for IGP frailty model is obtained directly from the unconditional CDF in (14), considering that the cumulative degradation $D(t)$ is equal to the degradation increment in the time interval from 0 up to t: $\Delta t \equiv [0, t]$. Then, we have

$$F_T(t) = P\left(D(t) \geq \rho\right) = 1 - F(y = \rho|g_{\boldsymbol{\theta}}(t),\eta,\boldsymbol{\alpha}). \tag{15}$$

The lifetime PDF is obtained from the derivative of (15) with respect to t:

$$f_T(t) = \frac{\partial F_T(t)}{\partial t}.$$

3.2 | Inference for unknown parameters in IGP frailty model

Considering n units observed at the inspection times t_{ij} $(j = 1, \ldots, n_i)$, leading to the observed degradation increments $y_{i1}, \ldots, y_{in_i}$ and z_i $(i = 1, \ldots, n)$ independent and identically distributed (IID) frailty variables with PDF $f_{\boldsymbol{\alpha}}(z_i)$, the complete likelihood function is given by

$$L(g_{\boldsymbol{\theta}}(t),\eta,\boldsymbol{z}) = \prod_{i=1}^{n}\prod_{j=1}^{n_i} h_i(y_{ij}|\Delta g_{\boldsymbol{\theta}}(t_{ij}),\eta,z_i)R_i(y_{ij}|\Delta g_{\boldsymbol{\theta}}(t_{ij}),\eta,z_i)f_{\boldsymbol{\alpha}}(z_i). \tag{16}$$

Hence, the unconditional likelihood function is obtained by integrating out the variable z_i:

$$L(g_{\boldsymbol{\theta}}(t),\eta,\boldsymbol{\alpha}) = \int_0^{\infty} L(g_{\boldsymbol{\theta}}(t),\eta,\boldsymbol{z})f_{\boldsymbol{\alpha}}(z_i)dz_i.$$

For the sake of clarity, we first obtain the partial likelihood function of each unit i:

$$L_i = \int_0^{\infty} \prod_{j=1}^{n_i} h_i(y_{ij}|\Delta g_{\boldsymbol{\theta}}(t_{ij}),\eta,z_i)R_i(y_{ij}|\Delta g_{\boldsymbol{\theta}}(t_{ij}),\eta,z_i)f_{\boldsymbol{\alpha}}(z_i)dz_i = L_{1i} \times L_{2i}, \tag{17}$$

where

$$L_{1i} = \prod_{j=1}^{n_i} h_{\text{IGP}}(y_{ij}|\Delta g_{\boldsymbol{\theta}}(t_{ij}),\eta),$$

$$L_{2i} = \int_0^{\infty} \left(\frac{1}{z_i}\right)^{n_i} \exp\left\{-\frac{1}{z_i}\sum_{j=1}^{n_i} H_{\text{IGP}}(y_{ij}|\Delta g_{\boldsymbol{\theta}}(t_{ij}),\eta)\right\} f_{\boldsymbol{\alpha}}(z_i)dz_i.$$

Note that the first term L_{1i} does not depend on frailty distribution and the second term L_{2i} depends on the assigned frailty distribution.

Thus, the likelihood function in (17) for n units is rewritten as

$$L(g_{\boldsymbol{\theta}}(t),\eta,\boldsymbol{\alpha}) = \prod_{i=1}^{n} L_{1i} \times L_{2i}$$

and the corresponding log-likelihood function is given by

$$\ell(g_{\boldsymbol{\theta}}(t),\eta,\boldsymbol{\alpha}) = \sum_{i=1}^{n} \log(L_{1i}) + \sum_{i=1}^{n} \log(L_{2i}). \tag{18}$$

The maximum likelihood estimates (MLEs) of the parameters are obtained by maximization of (18), and the confidence intervals can be constructed from asymptotic properties of the MLEs.

The individual frailties can be obtained using a Bayesian inference approach[27], where the frailty PDF for each unit i given the observed data is

$$f(z_i|\boldsymbol{Y}) \propto L(g_{\boldsymbol{\theta}}(t),\eta,\boldsymbol{z}),$$

where $L(g_{\boldsymbol{\theta}}(t),\eta,\boldsymbol{z})$ is given in (16) and the terms that do not depend on z_i are removed from the formula.

3.3 | Gamma distribution for frailty

In this section, we assume that z_i's are an IID sample from gamma distribution, which is one of the most popular distributions for modeling the frailty term[28]. In order to keep our model identifiable[29], we shall assume a gamma distribution with unitary mean and α variance for z_i, then we have

$$h_i(y|\Delta g_\theta(t), \eta, z_i) = \frac{1}{z_i} \times h_{\text{IGP}}(y|\Delta g_\theta(t), \eta), \tag{19}$$

where $z_i \sim \text{Gamma}\left(\frac{1}{\alpha}, \alpha\right)$ and

$$f_\alpha(z_i) = \frac{z_i^{\frac{1}{\alpha}-1} \alpha^{-\frac{1}{\alpha}} \exp\left\{-\frac{z_i}{\alpha}\right\}}{\Gamma\left(\frac{1}{\alpha}\right)},$$

with $\Gamma(\cdot)$ being the gamma function.

Model (19) is referred to as the IGP-gamma frailty model throughout the paper.

The unconditional reliability function of the degradation increments in IGP-gamma frailty model is given by

$$R(y|\Delta g_\theta(t), \eta, \boldsymbol{\alpha}) = \begin{cases} 0, \text{ if } R_{\text{IGP}}(y|\Delta g_\theta(t), \eta) = 0, \\ \dfrac{2\alpha^{-\frac{1}{\alpha}} \left(\alpha H_{\text{IGP}}(y|\Delta g_\theta(t), \eta)\right)^{\frac{1}{2\alpha}} A}{\Gamma\left(\frac{1}{\alpha}\right)}, \text{ if } 0 < R_{\text{IGP}}(y|\Delta g_\theta(t), \eta) < 1, \\ 1, \text{ if } R_{\text{IGP}}(y|\Delta g_\theta(t), \eta) = 1, \end{cases} \tag{20}$$

where $A = \text{BesselK}\left[\frac{1}{\alpha}, \frac{2\sqrt{H_{\text{IGP}}(y|\Delta g_\theta(t), \eta)}}{\sqrt{\alpha}}\right]$ and $\text{BesselK}[\nu, \xi]$ is the modified Bessel function of the second kind $K_\nu(\xi)$.

The unconditional CDF is easily obtained from (20) and the relation (14).

The lifetime CDF in IGP-gamma frailty model comes directly from (15), and the lifetime PDF is given by

$$f_T(t) = f_{T_{\text{IGP}}}(t) \times \frac{H_{\text{IGP}}(y = \rho|g_\theta(t), \eta) \left[\sqrt{\alpha H_{\text{IGP}}(y = \rho|g_\theta(t), \eta)}(A_1 + A_2) - A\right]}{\alpha^{\frac{1}{2\alpha}+1} \Gamma\left(\frac{1}{\alpha}\right) R_{\text{IGP}}(y = \rho|g_\theta(t), \eta)},$$

where $f_{T_{\text{IGP}}}(\cdot)$ is as given in (7), A is as given in (20), $A_1 = \text{BesselK}\left[-1 + \frac{1}{\alpha}, 2\frac{\sqrt{H_{\text{IGP}}(y|\Delta g_\theta(t), \eta)}}{\sqrt{\alpha}}\right]$ and $A_2 = \text{BesselK}\left[1 + \frac{1}{\alpha}, 2\frac{\sqrt{H_{\text{IGP}}(y|\Delta g_\theta(t), \eta)}}{\sqrt{\alpha}}\right]$.

The second term in (17) is given by

$$L_{2i} = \frac{2\alpha^{-\frac{1}{\alpha}} \left(\alpha \sum_{j=1}^{n_i} H_{\text{IGP}}(y_{ij}|\Delta g_\theta(t_{ij}), \eta)\right)^{\frac{1}{2\alpha} - \frac{n_i}{2}} A_{1i}}{\Gamma\left(\frac{1}{\alpha}\right)},$$

where $A_{1i} = \text{BesselK}\left[\frac{1}{\alpha} - n_i, 2\sqrt{\frac{\sum_{j=1}^{n_i} H_{\text{IGP}}(y_{ij}|\Delta g_\theta(t_{ij}), \eta)}{\alpha}}\right]$.

Therefore, the likelihood function for n units is

$$L(g_\theta(t), \eta, \alpha) = \prod_{i=1}^{n} \left[\prod_{j=1}^{n_i} h_{\text{IGP}}(y_{ij}|\Delta g_\theta(t_{ij}), \eta)\right] \frac{2\alpha^{-\frac{1}{\alpha}} \left(\alpha \sum_{j=1}^{n_i} H_{\text{IGP}}(y_{ij}|\Delta g_\theta(t_{ij}), \eta)\right)^{\frac{1}{2\alpha} - \frac{n_i}{2}} A_{1i}}{\Gamma\left(\frac{1}{\alpha}\right)}.$$

The corresponding log-likelihood function is

$$\ell(g_\theta(t),\eta,\alpha)=\sum_{i=1}^{n}\sum_{j=1}^{n_i}\log\left[h_{\text{IGP}}(y_{ij}|\Delta g_\theta(t_{ij}),\eta)\right]+\sum_{i=1}^{n}\log\left(A_{1i}\right)-n\log\left[\Gamma\left(\frac{1}{\alpha}\right)\right]+n\log(2)-\frac{n}{\alpha}\log(\alpha)$$
$$+\sum_{i=1}^{n}\left(\frac{1}{2\alpha}-\frac{n_i}{2}\right)\log\left[\alpha\sum_{j=1}^{n_i}H_{\text{IGP}}(y_{ij}|\Delta g_\theta(t_{ij}),\eta)\right].$$

The frailty for each unit i given the observed data belongs to Generalized IG (GIG) distribution, i.e.,

$$z_i|\boldsymbol{Y}\sim\text{GIG}\left(\frac{2}{\alpha},\,2\sum_{j=1}^{n_i}H_{\text{IGP}}(y_{ij}|\Delta g_\theta(t_{ij}),\eta),\,\frac{1}{\alpha}-n_i\right),$$

whose mean and variance are given by

$$E\left[z_i|\boldsymbol{Y}\right]=A_{2i}\sqrt{\alpha\sum_{j=1}^{n_i}H_{\text{IGP}}(y_{ij}|\Delta g_\theta(t_{ij}),\eta)},$$
$$Var\left[z_i|\boldsymbol{Y}\right]=(A_{3i}-A_{2i}^2)\alpha\sum_{j=1}^{n_i}H_{\text{IGP}}(y_{ij}|\Delta g_\theta(t_{ij}),\eta),$$

where $A_{2i}=\dfrac{\text{BesselK}\left[\frac{1}{\alpha}-n_i+1,\,A\right]}{\text{BesselK}\left[\frac{1}{\alpha}-n_i,\,A\right]}$, $A_{3i}=\dfrac{\text{BesselK}\left[\frac{1}{\alpha}-n_i+2,\,A\right]}{\text{BesselK}\left[\frac{1}{\alpha}-n_i,\,A\right]}$ and $A=2\sqrt{\dfrac{\sum_{j=1}^{n_i}H_{\text{IGP}}(y_{ij}|\Delta g_\theta(t_{ij}),\eta)}{\alpha}}$.

3.4 | IG distribution for frailty

Here, we suppose that z_i's are an IID sample from IG distribution with unitary mean and α variance. Then, we have

$$h_i(y|\Delta g_\theta(t),\eta,z_i)=\frac{1}{z_i}\times h_{\text{IGP}}(y|\Delta g_\theta(t),\eta),\tag{21}$$

where $z_i\sim\text{IG}\left(1,\frac{1}{\alpha}\right)$ and $f_\alpha(z_i)=\dfrac{1}{\sqrt{2\pi\alpha z_i^3}}\exp\left\{-\dfrac{(z_i-1)^2}{2\alpha z_i}\right\}$. Model (21) is referred to as the IGP-IG frailty model throughout the paper.

The unconditional reliability function of the degradation increments in IGP-IG frailty model is given by

$$R(y|\Delta g_\theta(t),\eta,\boldsymbol{\alpha})=\begin{cases}0,\ \text{if}\ R_{\text{IGP}}(y|\Delta g_\theta(t),\eta)=0,\\ \dfrac{e^{-\frac{1}{\alpha}\left(\sqrt{1+2\alpha H_{\text{IGP}}(y|\Delta g_\theta(t),\eta)}-1\right)}}{\sqrt{1+2\alpha H_{\text{IGP}}(y|\Delta g_\theta(t),\eta)}},\ \text{if}\ 0<R_{\text{IGP}}(y|\Delta g_\theta(t),\eta)<1,\\ 1,\ \text{if}\ R_{\text{IGP}}(y|\Delta g_\theta(t),\eta)=1.\end{cases}\tag{22}$$

The unconditional CDF is easily obtained from (22) and the relation (14).

The lifetime CDF in IGP-IG frailty model comes directly from (15), and the lifetime PDF is given by

$$f_T(t)=\frac{f_{T_{\text{IGP}}}(t)\,e^{-\frac{1}{\alpha}\left(\sqrt{1+2\alpha H_{\text{IGP}}(y=\rho|g_\theta(t),\eta)}-1\right)}}{R_{\text{IGP}}(y=\rho|g_\theta(t),\eta)\left[1+2\alpha H_{\text{IGP}}(y=\rho|g_\theta(t),\eta)\right]}\times\left[1+\frac{\alpha}{\sqrt{1+2\alpha H_{\text{IGP}}(y=\rho|g_\theta(t),\eta)}}\right],$$

where $f_{T_{\text{IGP}}}(\cdot)$ is as given in (7).

The second term in (17) is given by

$$L_{2i}=\sqrt{\frac{2}{\pi\alpha}}\left(\frac{1}{1+2\alpha\sum_{j=1}^{n_i}H_{\text{IGP}}(y_{ij}|\Delta g_\theta(t_{ij}),\eta)}\right)^{\frac{1}{4}+\frac{n_i}{2}}B_{1i}\exp\left\{\frac{1}{\alpha}\right\},$$

where $B_{1i} = \text{BesselK}\left[\frac{1}{2} + n_i, \frac{\sqrt{1 + 2\alpha \sum_{j=1}^{n_i} H_{\text{IGP}}(y_{ij}|\Delta g_\theta(t_{ij}), \eta)}}{\alpha}\right]$. The likelihood function for n units is

$$L(g_\theta(t), \eta, \boldsymbol{\alpha}) = \prod_{i=1}^{n} \left[\prod_{j=1}^{n_i} h_{\text{IGP}}(y_{ij}|\Delta g_\theta(t_{ij}), \eta)\right] \sqrt{\frac{2}{\pi\alpha}} B_{1i} \exp\left\{\frac{1}{\alpha}\right\} \left(\frac{1}{1 + 2\alpha \sum_{j=1}^{n_i} H_{\text{IGP}}(y_{ij}|\Delta g_\theta(t_{ij}), \eta)}\right)^{\frac{1}{4} + \frac{n_i}{2}}.$$

Hence, the corresponding log-likelihood function is

$$\begin{aligned}\ell(g_\theta(t), \eta, \alpha) = &\sum_{i=1}^{n} \sum_{j=1}^{n_i} \log\left[h_{\text{IGP}}(y_{ij}|\Delta g_\theta(t_{ij}), \eta)\right] + \frac{n}{\alpha} + \frac{n}{2}\log(2) - \frac{n}{2}\log(\pi) + \sum_{i=1}^{n} \log(B_{1i}) \\ &- \sum_{i=1}^{n} \left(\frac{1}{4} + \frac{n_i}{2}\right) \log\left(1 + 2\alpha \sum_{j=1}^{n_i} H_{\text{IGP}}(y_{ij}|\Delta g_\theta(t_{ij}), \eta)\right) - \frac{n}{2}\log(\alpha).\end{aligned}$$

The frailty for each unit i given the observed data belongs to the GIG distribution:

$$z_i|\boldsymbol{Y} \sim \text{GIG}\left(\frac{1}{\alpha}, 2\sum_{j=1}^{n_i} H_{\text{IGP}}(y_{ij}|\Delta g_\theta(t_{ij}), \eta) + \frac{1}{\alpha}, -\frac{3}{2} - n_i + 1\right),$$

whose mean and variance are given by

$$\begin{aligned}E\left[z_i|\boldsymbol{Y}\right] &= B_{2i}\sqrt{1 + 2\alpha \sum_{j=1}^{n_i} H_{\text{IGP}}(y_{ij}|\Delta g_\theta(t_{ij}), \eta)}, \\ Var\left[z_i|\boldsymbol{Y}\right] &= (B_{3i} - B_{2i}^2)\left(1 + 2\alpha \sum_{j=1}^{n_i} H_{\text{IGP}}(y_{ij}|\Delta g_\theta(t_{ij}), \eta)\right),\end{aligned}$$

where $B_{2i} = \dfrac{\text{BesselK}\left[-\frac{3}{2} - n_i + 2,\ B\right]}{\text{BesselK}\left[-\frac{3}{2} - n_i + 1,\ B\right]}$ and $B_{3i} = \dfrac{\text{BesselK}\left[-\frac{3}{2} - n_i + 3,\ B\right]}{\text{BesselK}\left[-\frac{3}{2} - n_i + 1,\ B\right]}$.

4 | SIMULATION STUDY

A simulation study was conducted based on the generation of 5,000 artificial datasets from IGP frailty model (11) with five different sample sizes: $n = 20$, 50, 100, 200 and 500. The values set to the parameters are grounded on the LASER data[30], in which the degradation paths have linear behavior. The components are measured from 0 to 4-time units with ten equidistant intervals. The parameter values are set as $g_\theta(t) = \theta t$ with $\theta = 2$, $\eta = 15$ and two scenarios for α: $\alpha = 0.05$, which represents small unobserved heterogeneity; and $\alpha = 0.5$, which describes moderate unobserved heterogeneity. Thus, we made inferences for the parameters in the IGP model (1) and IGP frailty model (11). In other words, we generated data with frailty and made inferences ignoring or not ignoring it. The MLEs of the model parameters, the coverage probabilities at level 95% (95% CPs), and the mean square errors of the MLEs (MSEs) under different models, frailty distributions and α values are discussed.

4.1 | Gamma distribution for frailty

Tables 1 and 2 show the MLEs, 95% CPs and MSEs under $\alpha = 0.05$ and $\alpha = 0.5$. It can be observed that the MLEs are closer to the corresponding true values as the sample size increases. In addition, we notice that as n grows, the MSEs are lower even when frailty is ignored. Nevertheless, the 95% CPs are far from the nominal value (95%) as n grows and frailty is ignored. Moreover, the MLEs of η in the IGP model are further from its true value as α increases, because η captures the intrinsic variability in the data.

TABLE 1 The MLEs, 95% CPs and MSEs under gamma frailty and $\alpha = 0.05$, which show that the estimates are closer to the corresponding true values as the sample size increases and the MSEs are lower even when frailty is ignored.

		IGP model (1)			IGP-gamma frailty model (19)		
n	True value	MLE	95% CP	MSE	MLE	95% CP	MSE
20	$\mu = 2$	1.9962	0.8918	0.0025	2.0022	0.9474	0.0025
	$\eta = 15$	14.6500	0.9060	3.1973	15.2750	0.9530	3.3901
	$\alpha = 0.05$	–	–	–	0.0588	0.9996	0.0017
50	$\mu = 2$	1.9953	0.8884	0.0010	2.0006	0.9428	0.0010
	$\eta = 15$	14.5820	0.8792	1.4056	15.1220	0.9506	1.3255
	$\alpha = 0.05$	–	–	–	0.0511	0.9640	0.0008
100	$\mu = 2$	1.9952	0.8888	0.0005	2.0003	0.9478	0.0005
	$\eta = 15$	14.5320	0.8636	0.8016	15.0490	0.9530	0.6222
	$\alpha = 0.05$	–	–	–	0.0490	0.9374	0.0005
200	$\mu = 2$	1.9948	0.8742	0.0003	1.9999	0.9478	0.0003
	$\eta = 15$	14.4950	0.7822	0.5590	15.0100	0.9520	0.3234
	$\alpha = 0.05$	–	–	–	0.0490	0.9362	0.0002
500	$\mu = 2$	1.9948	0.8482	0.0001	2.0000	0.9498	0.0001
	$\eta = 15$	14.4930	0.6128	0.3806	15.0160	0.9502	0.1300
	$\alpha = 0.05$	–	–	–	0.0497	0.9420	0.0001

TABLE 2 The MLEs, 95% CPs and MSEs under gamma frailty and $\alpha = 0.5$, which demonstrate that the estimates are closer to their corresponding true values as the sample size increases.

		IGP model (1)			IGP-gamma frailty model (19)		
n	True value	MLE	95% CP	MSE	MLE	95% CP	MSE
20	$\theta = 2$	1.9449	0.5708	0.0120	1.9931	0.9282	0.0097
	$\eta = 15$	11.7230	0.3476	15.8270	15.5660	0.9494	7.5449
	$\alpha = 0.5$	–	–	–	0.4622	0.8688	0.0295
50	$\theta = 2$	1.9452	0.4774	0.0067	1.9956	0.9394	0.0040
	$\eta = 15$	11.3570	0.0974	15.1910	15.2830	0.9522	2.8256
	$\alpha = 0.5$	–	–	–	0.4793	0.9142	0.0117
100	$\theta = 2$	1.9423	0.3302	0.0052	1.9935	0.9392	0.0020
	$\eta = 15$	11.2990	0.0124	14.6430	15.2630	0.9512	1.4586
	$\alpha = 0.5$	–	–	–	0.4843	0.9268	0.0060
200	$\theta = 2$	1.9444	0.1888	0.0040	1.9960	0.9454	0.0010
	$\eta = 15$	11.1980	0.0000	14.9140	15.1600	0.9534	0.7024
	$\alpha = 0.5$	–	–	–	0.4869	0.9372	0.0030
500	$\theta = 2$	1.9443	0.0310	0.0035	1.9961	0.9430	0.0004
	$\eta = 15$	11.1590	0.0000	14.9370	15.1330	0.9488	0.2870
	$\alpha = 0.5$	–	–	–	0.4891	0.9306	0.0013

4.2 | Inverse Gaussian distribution for frailty

Tables 3 and 4 present the MLEs, 95% CPs and MSEs under $\alpha = 0.05$ and $\alpha = 0.5$. Similarly to the results under gamma frailty, the MLEs are closer to their corresponding true values as n increases. For the IGP model, the MLEs of η are further from its true value as n and α grow, and the MLEs of θ keep close to its true value under different scenarios. Moreover, the MSEs decrease when n increases, but the 95% CPs are far from the nominal value when the presence of frailty is not included in the model.

TABLE 3 The MLEs, 95% CPs and MSEs under IG frailty and $\alpha = 0.05$, which confirm that the MLEs return good estimates for the parameters.

		IGP model (1)			IGP-IG frailty model (21)		
n	True value	MLE	95% CP	MSE	MLE	95% CP	MSE
20	$\mu = 2$	1.9982	0.8990	0.0024	2.0041	0.9494	0.0025
	$\eta = 15$	14.6330	0.8966	3.2672	15.2440	0.9518	3.4128
	$\alpha = 0.05$	–	–	–	0.0622	1.0000	0.0024
50	$\mu = 2$	1.9955	0.8926	0.0010	2.0007	0.9458	0.0010
	$\eta = 15$	14.5800	0.8768	1.4284	15.1010	0.9502	1.3303
	$\alpha = 0.05$	–	–	–	0.0520	0.9702	0.0010
100	$\mu = 2$	1.9951	0.8824	0.0005	2.0002	0.9458	0.0005
	$\eta = 15$	14.5370	0.8546	0.8378	15.0450	0.9436	0.6579
	$\alpha = 0.05$	–	–	–	0.0502	0.9404	0.0005
200	$\mu = 2$	1.9954	0.8742	0.0003	2.0004	0.9444	0.0003
	$\eta = 15$	14.5020	0.7814	0.5500	15.0030	0.9512	0.3174
	$\alpha = 0.05$	–	–	–	0.0494	0.9418	0.0003
500	$\mu = 2$	1.9949	0.8470	0.0001	2.0000	0.9468	0.0001
	$\eta = 15$	14.5050	0.6208	0.3710	15.0120	0.9490	0.1304
	$\alpha = 0.05$	–	–	–	0.0498	0.9474	0.0001

TABLE 4 The MLEs, 95% CPs and MSEs under IG frailty and $\alpha = 0.5$, which confirm that the estimates are closer to the corresponding true values when n increases.

		IGP model (1)			IGP-IG frailty model (21)		
n	True value	MLE	95% CP	MSE	MLE	95% CP	MSE
20	$\theta = 2$	1.9517	0.5930	0.0100	1.9906	0.9170	0.0092
	$\eta = 15$	12.6520	0.4958	11.6590	15.5960	0.9454	7.3162
	$\alpha = 0.5$	–	–	–	0.4631	0.8576	0.0537
50	$\theta = 2$	1.9512	0.4974	0.0055	1.9910	0.9332	0.0038
	$\eta = 15$	12.3140	0.2652	9.6202	15.3730	0.9506	2.8987
	$\alpha = 0.5$	–	–	–	0.4683	0.8926	0.0205
100	$\theta = 2$	1.9517	0.3960	0.0039	1.9921	0.9360	0.0019
	$\eta = 15$	12.1790	0.0888	9.1002	15.2710	0.9532	1.3951
	$\alpha = 0.5$	–	–	–	0.4728	0.9064	0.0107
200	$\theta = 2$	1.9514	0.2312	0.0031	1.9919	0.9424	0.0010
	$\eta = 15$	12.1280	0.0062	8.8019	15.2270	0.9536	0.7025
	$\alpha = 0.5$	–	–	–	0.4714	0.9056	0.0056
500	$\theta = 2$	1.9511	0.0450	0.0027	1.9917	0.9236	0.0005
	$\eta = 15$	12.1060	0.0000	8.6116	15.2210	0.9318	0.3302
	$\alpha = 0.5$	–	–	–	0.4729	0.9008	0.0026

5 | APPLICATION

In this section, we illustrate the potentiality of the proposed model with two real-world datasets. In the application with the LASER (Section 5.1) and crack size data (Section 5.2), we consider the next form for the mean function in IGP model: $g_\theta(t) = \theta t$, $\theta > 0$. The parameter estimation was performed by applying the Quasi-Newton optimization method via the Broyden-Fletcher-Goldfarb-Shanno (BFGS) algorithm (see, e.g., Broyden[31]). The values used to initialize this algorithm were achieved as follows:

- For the IGP model, the starting values for θ and η are taken from Peng[9], whereby the authors obtained the MLEs analytically;

- For the IGP frailty model, the starting values for θ and η are similar to the MLEs in the IGP model, and the starting value for α is equal to 1.

5.1 | The LASER data

Some gadgets for light amplification by stimulated emission of radiation (LASER) show degradation over time, which results in a decrease in the emitted light. This luminosity can be kept considerably constant with an increase in the operating current. When this current attains a very high value, it is considered that the unit has failed. Meeker and Escobar[30] presented a study with degradation data of 15 LASER units from Gallium Arsenide (GaAs) type, with observations made at 4,000 hours of operation, with 16 equidistant time intervals. The degradation measure for each unit is the percentage increase in the current over time, related to the nominal current, and a unit is considered to have failed when the degradation measure attains 10%. Figure 2 exhibits the degradation paths, indicating the critical value related to the failure.

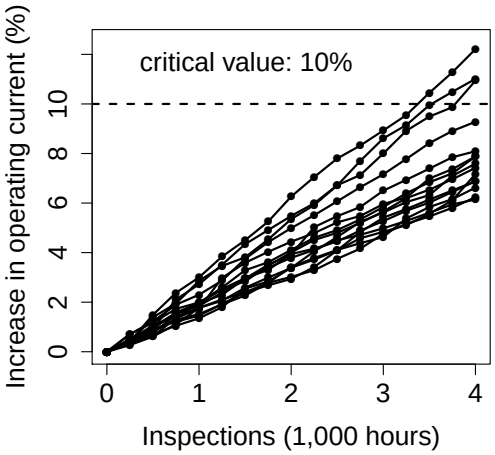

FIGURE 2 The degradation paths, indicating the critical value related to the failure of LASER devices.

Table 5 displays the MLEs, the standard errors of the MLEs (SEs) and the 95% confidence intervals (95% CIs) of the parameters under the IGP model, the IGP-gamma frailty model and the IGP-IG frailty model.

Since α must assume only positive values, we built the 95% CIs of α under a one-to-one parameter transformation[32]. More specifically, we first obtained the 95% CIs for $\log(\alpha)$ and then transformed them back into 95% CIs for α. For the sake of illustration, the time scale is expressed in 1,000 hours of operation, which means that the MLEs of θ need to be divided by 1,000 to be interpreted correctly.

In Table 5, it can be observed that the MLEs of the slope θ are identical in all models, whereas the MLEs of the scale parameter η are higher in both the IGP frailty models than in the IGP model because the variance α captures some of the intrinsic variability in the data. Moreover, we note that the SEs of θ and η in both IGP frailty models are higher than in the IGP model, which means that the SEs are significantly underestimated if we ignore the unobserved heterogeneity. This finding goes in the same line with Slimacek *et al.*[33,34], who also observed this effect in the variance when the presence of frailty is ignored.

We now assess the goodness-of-fit for the IGP model and IGP frailty model. Figure 3 shows the probability-probability plot (P-P plot) and quantile-quantile plot (Q-Q plot) along with the Anderson-Darling (AD) adherence test[35] of the observed degradation increments, from which we conclude that the IGP-based models are appropriate for these data because the dots in the plots are close to the diagonal line and the AD test's p-value is higher than 0.05.

In order to compare the fitted candidate models, we use the Akaike information criterion (AIC)[36] and the Bayesian information criterion (BIC)[37]. Table 6 shows these model selection criteria, from which we conclude that the IGP-IG frailty model best fitted the LASER data given that its AIC and BIC values are the lowest.

TABLE 5 The MLEs, SEs and 95% CIs for the parameters of the IGP, the IGP-gamma frailty and the IGP-IG frailty models based on the LASER data.

Model	Parameter	MLE	SE	95% CI
IGP (1)	θ	2.0372	0.0509	[1.9375 ; 2.1368]
	η	13.1300	1.3662	[10.4530 ; 15.8080]
IGP-gamma	θ	2.0510	0.1004	[1.8542 ; 2.2478]
frailty (19)	η	15.1480	2.3398	[10.5620 ; 19.7340]
	α	0.2104	0.0974	[0.0849 ; 0.5214]
IGP-IG	θ	2.0563	0.1076	[1.8455 ; 2.2671]
frailty (21)	η	15.1030	2.4479	[10.3050 ; 19.9010]
	α	0.2478	0.1265	[0.0911 ; 0.6742]

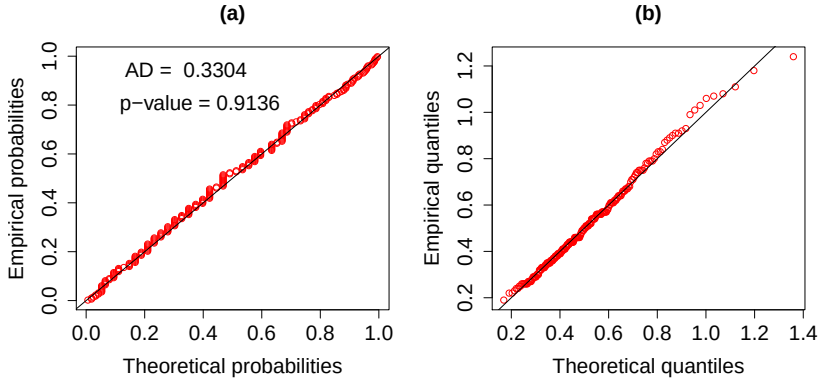

FIGURE 3 Goodness-of-fit test based on the LASER data: (a) IG P-P plot of the degradation increments and AD test, (b) IG Q-Q plot of the degradation increments, which confirms that the IGP-based models are appropriate for these data.

TABLE 6 The AIC and BIC values, from which the IGP-IG frailty model provides the best fit to the LASER data.

Model	AIC	BIC
IGP (1)	−146.1	−144.7
IGP-gamma frailty (19)	−174.6	−172.5
IGP-IG frailty (21)	−175.8	−173.7

Furthermore, the MLEs of the expected individual frailties ($\widehat{E\left[z_i|\boldsymbol{Y}\right]}$) are shown together with cumulative degradation values in Table 7, where the four most fragile components are highlighted in gray with their corresponding frailty estimates. We notice that the highest averages are directly related to the highest cumulative degradation values and vice versa. For illustrative purposes, Figure 4 displays the degradation paths from the LASER data with the information from Table 7.

Finally, Table 8 shows the MLEs of the lifetime quantiles and their corresponding 95% CIs for threshold $\rho = 10\%$, from which we notice that the quantile MLEs in IGP frailty model are lower than in IGP model, and their 95% CIs in IGP frailty model are wider than in IGP model.

TABLE 7 Cumulative degradation values and MLEs of the expected individual frailties based on the LASER data.

		$\widehat{E\left[z_i \mid \boldsymbol{Y}\right]}$	
Unit	Cumulative degradation	IGP-gamma frailty model (19)	IGP-IG frailty model (21)
1	10.94	1.6902	1.7355
2	9.28	1.2311	1.2184
3	6.88	0.6805	0.6651
4	6.14	0.5589	0.5556
5	7.59	0.8659	0.8420
6	11.01	1.6993	1.7460
7	7.17	0.8343	0.8114
8	6.24	0.4995	0.5036
9	7.88	0.8950	0.8705
10	12.21	1.9484	2.0426
11	7.42	0.7611	0.7404
12	7.88	0.9892	0.9655
13	8.09	1.0230	0.9999
14	6.88	0.6973	0.6808
15	6.62	0.6339	0.6225

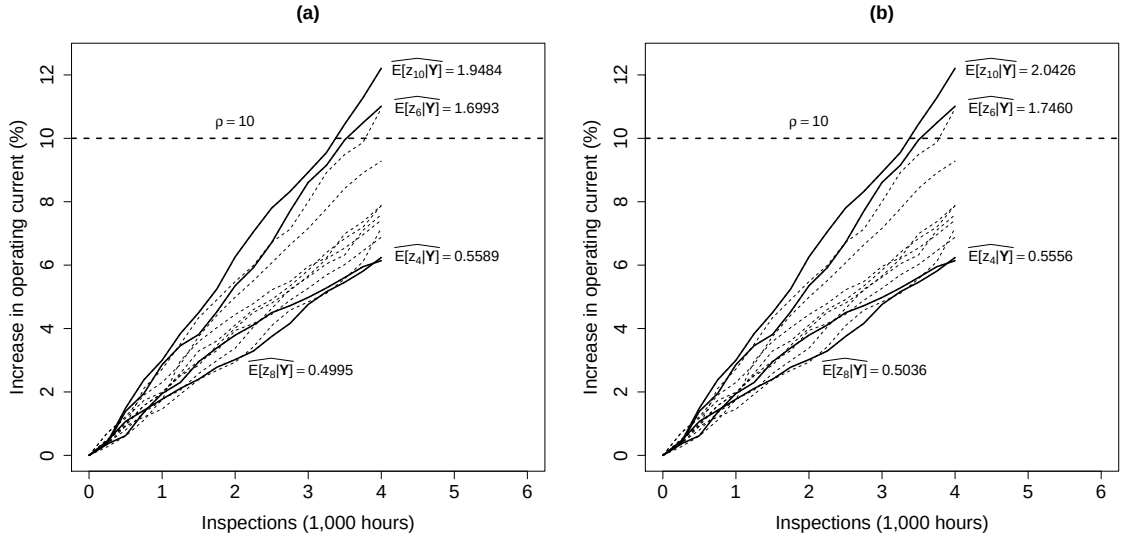

FIGURE 4 Degradation paths from the LASER data and MLEs of the expected individual frailties under different models: (a) IGP-gamma frailty model, (b) IGP-IG frailty model.

Figure 5 displays the charts of the lifetime CDF and PDF for the LASER components, from which we observe that the lifetime distributions for IGP model and IGP frailty model are unimodal and symmetrical, and the IGP frailty model concentrates more probability mass around the median than the IGP model without frailty term.

TABLE 8 The MLEs and 95% CIs of the lifetime quantiles based on the LASER data.

Model	Quantile	MLE	95% CI
IGP (1)	$t_{0.01}$	3.9341	[3.6806 ; 4.1877]
	$t_{0.05}$	4.2250	[3.9788 ; 4.4712]
	$t_{0.1}$	4.3801	[4.1367 ; 4.6234]
	$t_{0.5}$	4.9274	[4.6881 ; 5.1667]
	$t_{0.8}$	5.2870	[5.0450 ; 5.5289]
IGP-gamma frailty (19)	$t_{0.01}$	3.8242	[3.2975 ; 4.3509]
	$t_{0.05}$	4.1876	[3.6924 ; 4.6827]
	$t_{0.1}$	4.3671	[3.8834 ; 4.8508]
	$t_{0.5}$	4.9365	[4.4766 ; 5.3963]
	$t_{0.8}$	5.2733	[4.8218 ; 5.7248]
IGP-IG frailty (21)	$t_{0.01}$	3.7917	[3.1956 ; 4.3879]
	$t_{0.05}$	4.1748	[3.6377 ; 4.7118]
	$t_{0.1}$	4.3587	[3.8420 ; 4.8755]
	$t_{0.5}$	4.9266	[4.4461 ; 5.4071]
	$t_{0.8}$	5.2595	[4.7879 ; 5.7311]

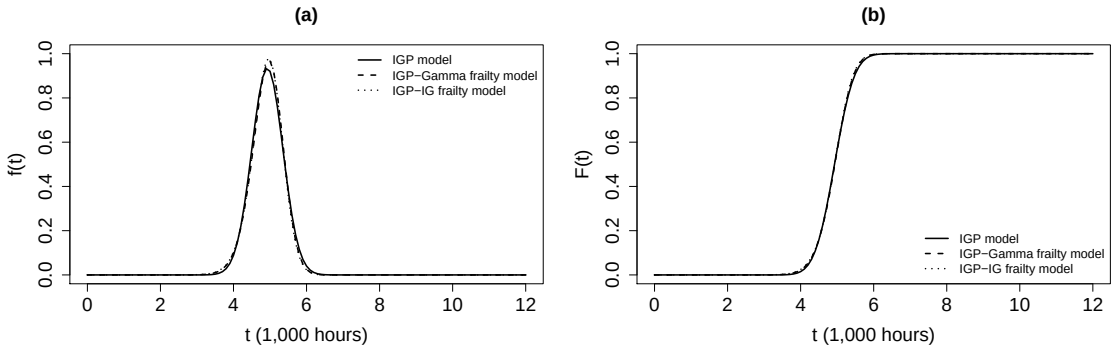

FIGURE 5 Lifetime distribution based on the LASER data: (a) Lifetime PDF, (b) Lifetime CDF.

5.2 | The crack size data

The fatigue crack size data introduced by Hudak *et al.*[38] were collected to obtain the fatigue cracks as a function of the number of cycles of applied stress for 21 test specimens. The data were exploited by Lu and Meeker[39] as a motivational example in the setting of nonlinear mixed-effects models for degradation data. There are 21 sample paths, one for each of the 21 test units, the test ends after 0.12 million cycles, and a threshold value of 1.6 inches is established to ascertain soft failures. Figure 6(a) exhibits the degradation paths, indicating the critical value related to the failure.

We performed the following transformation: $D^*(t) = \log\left(\frac{D(t)}{0.9}\right)$, proposed by Lu and Meeker[39] as a special case of Paris Law largely used to describe the growth of fatigue cracks in materials. Such transformation satisfies $D(0) = 0$ in the IGP model (1) and leaves the degradation paths close to the linear behavior. Figure 6(b) presents the transformed degradation paths from the crack size data, with the corresponding threshold ρ under the transformed data.

Table 9 shows the MLEs, SEs and 95% CIs of the parameters under different IGP models. Likewise the application with the LASER data, the 95% CIs of α are achieved under the exponential parameter transformation. For easy viewing, the unit scale of cycles is reported in $1,000$ cycles, then the MLEs of θ must be divided by $1,000$ in practice.

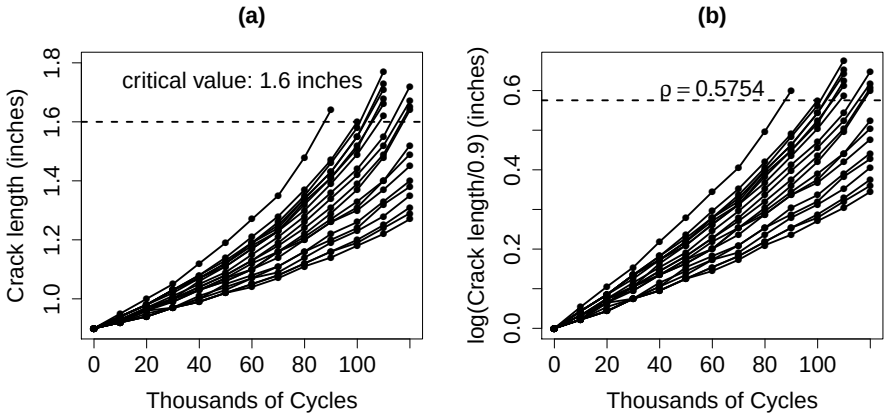

FIGURE 6 Degradation paths from the crack size data: (a) original data, (b) transformed data.

TABLE 9 The MLEs, SEs and 95% CIs for the parameters of the IGP, IGP-gamma frailty and IGP-IG frailty models based on the crack size data.

Model	Parameter	MLE	SE	95% CI
IGP (1)	θ	0.0047	0.0001	[0.0044 ; 0.0049]
	η	125.6900	13.2510	[99.7160 ; 151.6600]
IGP-gamma	θ	0.0049	0.0003	[0.0044 ; 0.0055]
frailty (19)	η	145.5500	24.8930	[96.7630 ; 194.3400]
	α	0.4160	0.1454	[0.2097 ; 0.8252]
IGP-IG	θ	0.0050	0.0004	[0.0042 ; 0.0058]
frailty (21)	η	138.7500	30.3990	[79.1680 ; 198.3300]
	α	0.7227	0.3702	[0.2648 ; 1.9721]

In Table 9, it can be observed that the MLE of α is lower in the IGP-gamma frailty model than in the IGP-IG frailty model, as well as its SE.

Figure 7 shows the P-P plot and Q-Q plot with the AD test of the observed degradation increments, from which we conclude that the IGP-based models are appropriate for these data (p-value > 0.05).

Furthermore, Table 10 shows the AIC and BIC estimates, from which we conclude that the IGP-gamma frailty model best fitted the crack size data given that its AIC and BIC values are the smallest.

TABLE 10 The AIC and BIC values, which reveal that the IGP-gamma frailty model has the best fit for the crack size data.

Model	AIC	BIC
IGP (1)	$-1,270.4$	$-1,268.4$
IGP-gamma frailty (19)	$-1,316.7$	$-1,313.5$
IGP-IG frailty (21)	$-1,314.1$	$-1,310.9$

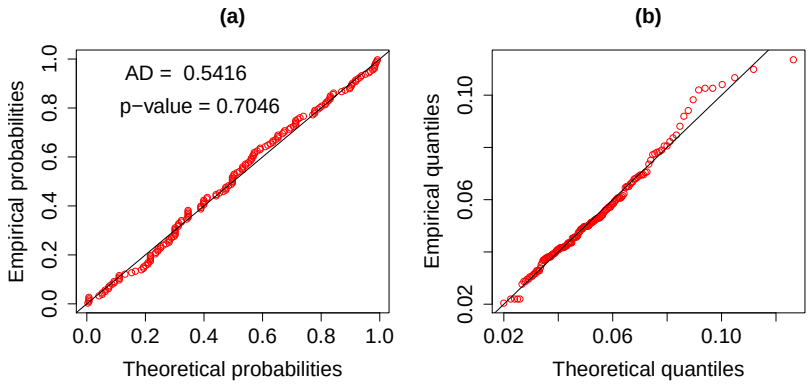

FIGURE 7 Goodness-of-fit test based on the crack size data: (a) IG P-P plot of the degradation increments and AD test, (b) IG Q-Q plot of the degradation increments, which confirms that the IGP-based models are appropriate for these data.

In order to analyze the individual frailties, Table 11 shows the MLEs of the expected individual frailties ($\widehat{E\left[z_i|\boldsymbol{Y}\right]}$) with the matching cumulative degradation values. The two most fragile components and the two less fragile components are highlighted in gray. Generally, the highest means are directly related to the highest cumulative degradation values. Figure 8 shows the degradation paths from the crack size data with the four components featured in Table 11. It is worth mentioning that the frailty model takes into account the cumulative damage related to the observation time, e.g., unit 1 does not have the highest degradation value, but it was the first unit to attain the threshold value and did not remain until the end of the experiment.

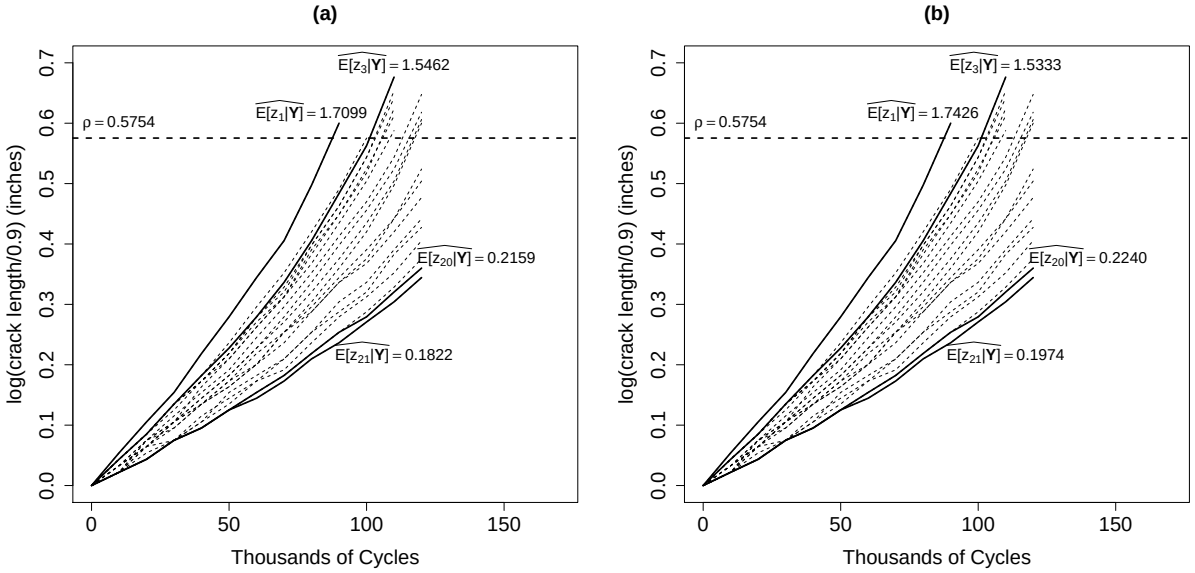

FIGURE 8 Degradation paths from the crack size data and MLEs of the expected individual frailties under different models: (a) IGP-gamma frailty model, (b) IGP-IG frailty model.

Finally, Table 12 presents the MLEs of the lifetime quantiles with their corresponding 95% CIs considering the critical value $\rho = 0.5754$, under transformed data. Besides, Figure 9 displays the charts of the lifetime CDF and PDF for the components.

TABLE 11 Cumulative degradation values and MLEs of the expected individual frailties based on the crack size data.

		$\widehat{E\left[z_i \mid \boldsymbol{Y}\right]}$	
Unit	Cumulative degradation	IGP-gamma frailty model (19)	IGP-IG frailty model (21)
1	0.6001	1.7099	1.7426
2	0.5754	1.3346	1.2963
3	0.6763	1.5462	1.5333
4	0.6535	1.4607	1.4354
5	0.6419	1.4150	1.3838
6	0.6242	1.3460	1.3066
7	0.6122	1.2825	1.2367
8	0.5878	1.1921	1.1387
9	0.6477	1.2540	1.2044
10	0.6182	1.1344	1.0772
11	0.6061	1.0876	1.0283
12	0.6001	1.1138	1.0554
13	0.5241	0.8345	0.7728
14	0.4769	0.5585	0.5145
15	0.5041	0.6800	0.6257
16	0.4418	0.4864	0.4501
17	0.4274	0.4726	0.4379
18	0.4055	0.3813	0.3594
19	0.3754	0.2637	0.2623
20	0.3600	0.2159	0.2240
21	0.3444	0.1822	0.1974

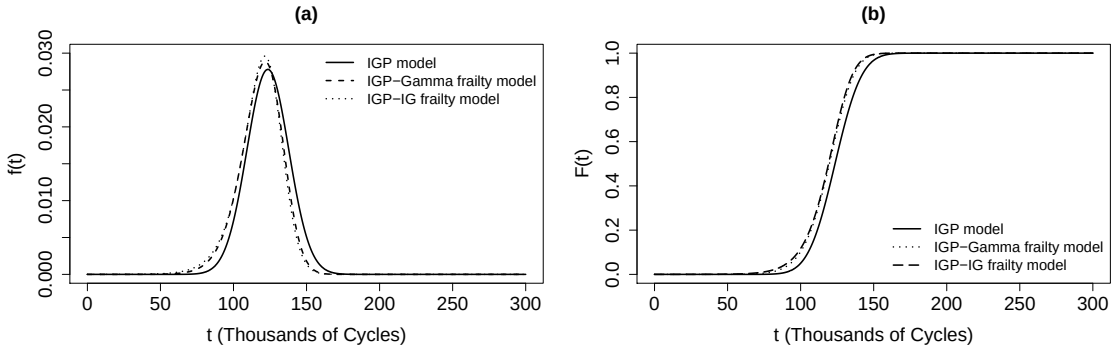

FIGURE 9 Lifetime distribution based on the crack size data: (a) Lifetime PDF, (b) Lifetime CDF.

From Table 12 and Figure 9, we can observe that the PDF and CDF for IGP-gamma frailty model and IGP-IG frailty model are similar to each other and differ from IGP model. Moreover, the presence of the frailty term slightly offsets the PDF to the left, which means that the time-to-failure is supposed to be lower in IGP frailty model than in IGP model.

TABLE 12 The MLEs and 95% CIs of the lifetime quantiles based on the crack size data.

Model	Quantile	MLE	95% CI
IGP (1)	$t_{0.01}$	90.1820	[83.2820 ; 97.0810]
	$t_{0.05}$	99.9390	[93.3300 ; 106.5500]
	$t_{0.1}$	105.1500	[98.6510 ; 111.6400]
	$t_{0.5}$	123.5300	[117.1900 ; 129.8700]
	$t_{0.8}$	135.6100	[129.1500 ; 142.0700]
IGP-gamma frailty (19)	$t_{0.01}$	79.5580	[63.2580 ; 95.8580]
	$t_{0.05}$	93.1770	[78.2890 ; 108.0700]
	$t_{0.1}$	99.7460	[85.3810 ; 114.1100]
	$t_{0.5}$	119.7200	[106.4000 ; 133.0300]
	$t_{0.8}$	130.8500	[117.8500 ; 143.8500]
IGP-IG frailty (21)	$t_{0.01}$	73.9050	[48.5510 ; 99.2590]
	$t_{0.05}$	90.6790	[69.9360 ; 111.4200]
	$t_{0.1}$	98.2260	[79.0710 ; 117.3800]
	$t_{0.5}$	119.0800	[102.4700 ; 135.7000]
	$t_{0.8}$	129.8900	[113.6100 ; 146.1600]

6 | CONCLUDING REMARKS

In this paper, we proposed a frailty-based approach to estimate the IGP model for degradation data. The motivation here was that the frailty model might be more suitable to account for heterogeneity and natural interpretation. We assumed gamma and IG distributions for frailty. The methodology was implemented by using the Quasi-Newton optimization method via the BFGS algorithm available in Ox software[40] to achieve the MLEs of the model parameters. The algorithm reached convergence in the simulation study and in the application with two real datasets. The simulation study revealed that the asymptotic properties of the MLEs are compromised when we ignore the presence of frailty: the MSEs are small with large sample sizes, but the CPs are not close to the nominal value (95%), which means that the asymptotic intervals are not propitious to use. Finally, in the application with the LASER data and the crack size data, the IGP-IG and IGP-gamma frailty models presented results similar to each other; the former best fitted the LASER data whereas the latter best fitted the crack size data.

There is a large number of possible extensions of this current work. The proposed IGP frailty model can be extended to other distributions for frailty, for example, we may assign the Weibull distribution for frailty, following a similar approach as in Asha *et al.*[41]; the Birnbaum-Saunders distribution can also be considered for frailty, as discussed in Leão *et al.*[42]. Our approach should be investigated further in these contexts.

ACKNOWLEDGMENT

We are grateful to the anonymous referees and the associate editor for the very useful comments and suggestions, which greatly improved this paper. Pedro L. Ramos acknowledges support from to the São Paulo State Research Foundation (FAPESP Proc. 2017/25971-0). Francisco Louzada is supported by the Brazilian agencies CNPq (grant number 301976/2017-1) and FAPESP (grant number 2013/07375-0).

References

1. Lehmann A. *Failure Time Models Based on Degradation Processes*: 209–233; Boston, MA: Birkhäuser Boston . 2010.
2. Doksum KA. Degradation rate models for failure time and survival data. *CWI Quarterly* 1991; 4: 195–203.

3. Wang X. Wiener processes with random effects for degradation data. *Journal of Multivariate Analysis* 2010; 101(2): 340–351.

4. Lawless J, Crowder M. Covariates and Random Effects in a Gamma Process Model with Application to Degradation and Failure. *Lifetime Data Analysis* 2004; 10(3): 213–227.

5. Esary J, Marshall AW. Shock Models and Wear Processes. *The Annals of Probability* 1973; 1(4): 627-649.

6. Wasan MT. On an inverse Gaussian process. *Scandinavian Actuarial Journal* 1968; 1968(1-2): 69-96.

7. Wang X, Xu D. An Inverse Gaussian Process Model for Degradation Data. *Technometrics* 2010; 52(2): 188-197.

8. Ye ZS, Chen N. The Inverse Gaussian Process as a Degradation Model. *Technometrics* 2014; 56(3): 302-311.

9. Peng CY. Inverse Gaussian Processes With Random Effects and Explanatory Variables for Degradation Data. *Technometrics* 2015; 57(1): 100–111.

10. Qin H, Zhang S, Zhou W. Inverse Gaussian process-based corrosion growth modeling and its application in the reliability analysis for energy pipelines. *Frontiers of Structural and Civil Engineering* 2013; 7(3): 276–287.

11. Liu Z, Ma X, Yang J, Zhao Y. Reliability Modeling for Systems with Multiple Degradation Processes Using Inverse Gaussian Process and Copulas. *Mathematical Problems in Engineering* 2014; 1: 1-10.

12. Proschan F. Theoretical Explanation of Observed Decreasing Failure Rate. *Technometrics* 1963; 5(3): 375–383.

13. Zhang Z, Si X, Hu C, Kong X. Degradation modeling–based remaining useful life estimation: A review on approaches for systems with heterogeneity. *Proceedings of the Institution of Mechanical Engineers, Part O: Journal of Risk and Reliability* 2015; 229(4): 343-355. doi: 10.1177/1748006X15579322

14. Vaupel JW, Manton KG, Stallard E. The impact of heterogeneity in individual frailty on the dynamics of mortality. *Demography* 1979; 16(3): 439–454.

15. Lindqvist BH. On the Statistical Modeling and Analysis of Repairable Systems. *Statist. Sci.* 2006; 21(4): 532–551. doi: 10.1214/088342306000000448

16. Oakes D. Bivariate Survival Models Induced by Frailties. *Journal of the American Statistical Association* 1989; 84(406): 487-493.

17. Hougaard P. Survival Models for Heterogeneous Populations Derived from Stable Distributions. *Biometrika* 1986; 73(2): 387–396.

18. Unkel S, Farrington CP. A new measure of time-varying association for shared frailty models with bivariate current status data. *Biostatistics* 2012; 13(4): 665-679.

19. Lin J, Pulido J, Asplund M. Analysis for locomotive wheels' degradation. In: ; 2014: 1-7.

20. Lin J, Asplund M. Comparison study of heavy haul locomotive wheels' running surfaces wearing. *Eksploatacja i Niezawodność* 2014; 16(2): 276–287.

21. Ibe OC. *Markov Processes for Stochastic Modeling*. Newnes. 2 ed. 2013.

22. Ibe OC. *Fundamentals of Applied Probability and Random Processes*. Academic Press. 2 ed. 2014.

23. Noortwijk vJ. A survey of the application of gamma processes in maintenance. *Reliability Engineering & System Safety* 2009; 94(1): 2–21.

24. Clayton DG. A model for association in bivariate life tables and its application in epidemiological studies of familial tendency in chronic disease incidence. *Biometrika* 1978; 65(1): 141-151.

25. Cox DR. Regression Models and Life-Tables. *Journal of the Royal Statistical Society. Series B (Methodological)* 1972; 34(2): 187-220.

26. Abramowitz M, Stegun IA. *Laplace Transforms*ch. 29: 1019-1030; New York: Dover . 1972.

27. Gelman A, Carlin JB, Stern HS, Rubin DB. *Bayesian data analysis*ch. 1: 3-28; Boca Raton, FL, USA: Chapman & Hall/CRC. third ed. 2014.

28. Nielsen GG, Gill RD, Andersen PK, Sørensen TIA. A Counting Process Approach to Maximum Likelihood Estimation in Frailty Models. *Scandinavian Journal of Statistics* 1992; 19(1): 25-43.

29. Chris Elbers GR. True and Spurious Duration Dependence: The Identifiability of the Proportional Hazard Model. *The Review of Economic Studies* 1982; 49(3): 403-409.

30. Meeker WQ, Escobar LA. *Statistical Methods for Reliability Data*. New York: John Wiley & Sons . 1998.

31. Broyden CG. The convergence of a class of double-rank minimization algorithms. *Journal of the Institute of Mathematics and Its Applications* 1970; 6(1): 76–90.

32. Kalbfleisch JD. *Probability and Statistical Inference - Volume 2: Statistical Inference*. Springer-Verlag New York . 1985.

33. Slimacek V, Lindqvist BH. Nonhomogeneous Poisson process with nonparametric frailty. *Reliability Engineering & System Safety* 2016; 149: 14–23.

34. Slimacek V, Lindqvist BH. Nonhomogeneous Poisson process with nonparametric frailty and covariates. *Reliability Engineering & System Safety* 2017; 167: 75–83.

35. Marsaglia G, Marsaglia J. Evaluating the Anderson-Darling Distribution. *Journal of Statistical Software* 2004; 9(2): 1–5.

36. Sakamoto Y, Ishiguro M, Kitagawa G. *Akaike information criterion statistics*. 1. Springer Netherlands. 1 ed. 1986.

37. Schwarz G. Estimating the Dimension of a Model. *The Annals of Statistics* 1978; 6(2): 461–464.

38. Hudak Jr S, Saxena A, Bucci R, Malcolm R. Development of standard methods of testing and analyzing fatigue crack growth rate data. tech. rep., 1978.

39. Lu CJ, Meeker WQ. Using Degradation Measures to Estimate a Time-to-Failure Distribution. *Technometrics* 1993; 35(2): 161-174.

40. Doornik JA. An Object-Oriented Matrix Programming Language Ox 6.. 2009.

41. Asha G, Raja AV, Ravishanker N. Reliability modelling incorporating load share and frailty. *Applied Stochastic Models in Business and Industry* 2018; 34(2): 206–223.

42. Leão J, Leiva V, Saulo H, Tomazella V. Incorporation of frailties into a cure rate regression model and its diagnostics and application to melanoma data. *Statistics in Medicine* 2018; 37(29): 4421–4440.

AUTHOR BIOGRAPHIES

Lia Hanna Martins Morita is a Professor at the University of Mato Grosso, Brazil. She received her Ph.D. in Statistics from University Federal of São Carlos, Brazil. Her main areas of interest include Survival Analysis, Degradation Models, Regression Models, and Statistical Inference.

Vera Tomazella is a Professor of Statistics at University Federal of São Carlos, Brazil. Her main interests are survival analysis, Applied Statistical Genetics, Regression Model and statistical inference. She is Ph.D. from University of São Paulo, Brasil. Postdoctoral (Bayesian Reference Analysis), Universitat de Valencia- Spain and Postdoctoral (Survival Analysis), University of Manchester, Manchester-UK. She is joint author of 50 publications in statistical peer reviewed journals and 3 book chapters. She is Editor-in-Chief Technical Report of the Department of Statistics at UFSCar and Member of the Editorial board of the Revista Brasileira de Estatística – RBEs. Elected member of the International Statistical Institute (ISI) and member of the IBS Education Committee. More details can be found in http://www.servidores.ufscar.br/vera/en/index.php.

Narayanaswamy Balakrishnan received his BSc and MSc degrees in Statistics from the University of Madras, India, in 1976 and 1978, respectively. He finished his PhD in Statistics from the Indian Institute of Technology, Kanpur, India, in 1981. He is a distinguished university professor at McMaster University, Hamilton, ON, Canada. His research interests include distribution theory, ordered data analysis, censoring methodology, reliability, survival analysis, nonparametric inference, and statistical quality control. Professor Balakrishnan is a fellow of the American Statistical Association and a fellow of the Institute of Mathematical Statistics. He is currently the editor in chief of Communications in Statistics.

Pedro Luiz Ramos is a Postdoctoral Fellow at the Institute for Mathematical Science and Computing, University of São Paulo (USP), Brazil. He received his Ph.D. degree in Statistics from the University of São Paulo in 2018, his M.S. degree in Applied and Computational Mathematic from the São Paulo State University, Brazil, and his B.S. degree in Statistics from the same university. His main research interests are in survival analysis, Bayesian inference, classical inference, and probability distribution theory.

Paulo Henrique Ferreira is a Professor of Statistics at the Institute of Mathematics and Statistics, Federal University of Bahia (UFBA), Brazil. He received his Ph.D., M.Sc. and B.Sc. degrees in Statistics all from the Federal University of São Carlos (UFSCar), Brazil. He also has a Postdoctoral training at the University of São Paulo (USP), Brazil. His main research interests include survival and reliability analysis, data mining and statistical process control.

Francisco Louzada is a Full Professor of Statistics at the Institute for Mathematical Science and Computing, University of São Paulo (USP), Brazil. He received his Ph.D. degree in Statistics from the University of Oxford, UK, his M.Sc. degree in Computational Mathematics from USP, Brazil, and his B.Sc. degree in Statistics from UFSCar, Brazil. His main research interests are in survival analysis, data mining, Bayesian inference, classical inference, and probability distribution theory.

How to cite this article: L.H.M. Morita, V.L. Tomazella, N. Balakrishnan P.L. Ramos, P.H. Ferreira, and F. Louzada (2019), Inverse Gaussian Process Model with Frailty Term in Reliability Analysis, *Quality and Reliability Engineering International*, *2019; 00:1–15*.